Surface Roughness Measurement and Surface Smoothing via Phase-Contrast Imaging and either Grayscale Lithography or Laser Ablation

Kenneth C. Johnson, August 1, 2021

[Changes from the May 27, 2021 version: The title and abstract have been revised and the "August 1, 2021 Addendum" has been added.]

Abstract

Surface roughness can be measured by using a phase-contrast, point-imaging system to measure the surface height at a focal point relative to an average surface height across an area surrounding the point. A scanning process (e.g., raster scanning or turning) is used to construct a surface height profile over an extended area. At the same time, a surface smoothing process can be applied by a grayscale lithographic process in which a photoresist-coated surface is exposed to a laser-writing beam, which is intensity-modulated in response to the surface height measurement. Alternatively, surface smoothing can be effected by direct laser ablation of the surface.

Overview

Advanced optical systems for applications such as extreme ultraviolet (EUV) lithography require Angstrom-scale surface form and finish tolerances over apertures up to 1 meter in size. [1] High-spatial-frequency surface roughness can be substantially eliminated with polishing, and low-spatial-frequency errors can be corrected with ion-beam finishing, but mid-spatial-frequency errors in the range of approximately 1 μm to 1 mm cannot be easily corrected.

Optical lithography is well suited for patterning structures in the 1 μm to 1 mm range, and lithography methods that are used for fabricating diffraction optics on curves surfaces could be adapted for surface smoothing. [2, 3] New photoresist technologies and processes similar to the LAM Research dry resist might be useful for this application. [4] The material removal for smoothing applications would be quite small, e.g., in the range of 0.1 nm to 10 nm for EUV optics, which might necessitate a relatively thin resist. However, the corrective pattern would not necessarily need to be etched directly into the substrate; it could be etched into a sacrificial layer and subsequently transferred into the substrate. The differential etch rate between the sacrificial layer and the substrate can be controlled to scale down the etch depth in a manner similar to processes that are used for synchrotron grating fabrication. [5, 6]

The lithographic exposure can be done with a laser-writing system such as a lathe-type instrument with a focused laser beam replacing the cutting tool. The exposure dose can be controlled by an interferometric surface-roughness measuring system, which measures the surface height at each point relative to an average height over an area surrounding the point. The surface profile measurement and laser writing can be done as separate, sequential processes, or could be performed concurrently, with the profile measurement controlling the laser modulation in real time.

The lithographic patterning system could be used to also correct the surface form (low-spatial-frequency errors), based on a full-aperture interferometric map of the surface shape error. The form correction and surface smoothing can be done as separate processes, or could be done concurrently, with the interferometric measurement system providing control for smoothing while a pre-programed correction for the form error is added to the roughness correction.

Optical design

The interferometric surface-profiling system can be based on acousto-optic heterodyning, similar to the optical system described in Ref. 7, Figure 1 (with possible variations shown in Figures 5 and 6), but the optics following the optical fibers (the tool post assembly) are replaced by the apparatus illustrated in Figures 1 and 2 herein. Frequency-shifted laser radiation is conveyed to the apparatus by two polarization-preserving optical fibers – fiber 1 for the probe beam and fiber 2 for the reference beam – and the reflected radiation is conveyed back through the fibers to the detection sensors, as described in Ref. 7. The beam paths from the two fibers are merged by a polarizing beam splitter. Figure 1 illustrates a schematic ray trace from fiber 1 to the focal point on an inspection surface, and Figure 2 shows a schematic ray trace from fiber 2 to an annular illumination area surrounding the focal point. The ray traces represent bidirectional beam paths; the reflected radiation in each path is directed back into the corresponding fiber. The focusing elements are schematically illustrated as refracting lenses in Figures 1 and 2, but could have alternative forms such as planar, phase-Fresnel diffractive lenses.

Figure 3 illustrates the focus patterns on the inspection surface for the probe beam and the reference beam. The probe beam is focused onto the surface at high numerical aperture (NA) to achieve a high-resolution focus spot (Figure 1). The reference beam can be focused at low NA to increase the beam area coverage (Figure 2); in addition, a phase-modifying optical surface such as a binary diffractive axicon [8] can be interposed in the reference beam path to spread the focused illumination into an annular ring covering a larger area. The diffractive axicon is a circular, binary phase grating with a zone pattern having the form illustrated in Figure 4.

The surface is scanned, e.g., in a raster pattern or by turning it on a lathe-type instrument, to acquire profilometry data over an extended area. Accurate focus control must be maintained while scanning, and the apparatus can be adapted to provide autofocus control as illustrated in Figure 5. A partially-reflecting beam splitter is interposed in the probe beam path to divert a portion of the beam power on the return path through a focusing lens. A diffraction grating on the beam splitter divides the beam power between two foci on the lens focal plane, and two focus-sensor optical fibers are positioned at the foci. (The grating zone pattern is illustrated in Figure 6.) The fibers are slightly displaced from the focal plane, one above the plane and the other below, so that the detector signals acquired from the two fibers provide an accurate measure of focus error. The autofocus system dynamically controls the inspection surface height to keep the two signals in balance. (Other design variants for autofocus include astigmatic focus error detection. [9, 10])

The autofocus will keep the probe beam accurately in focus, but on a curved surface the reference beam will be slightly out of focus and phase-shifted due to the surface curvature. The surface height measurement at the probe point can be corrected based on the known base surface

curvature. In addition, if the curvature-induce phase shift is large and varies across the reference beam, it could be advantageous to correct it optically by incorporating focus control in the reference beam path. One or more lens elements in the reference beam path can be moved to compensate for non-flatness of the inspection surface, including asymmetric (e.g., saddle-shape) curvature.

The optics can be further adapted to perform laser writing on a photoresist-coated surface concurrently with surface profile height sensing. The exposure beam, from a modulated laser source, can be merged into the probe beam's optical path by means of a dichroic beam splitter as illustrated in Figure 7. Typically, a short-wavelength laser (blue or UV) would be used for exposure while a longer wavelength, which does not affect the resist, is used for surface profiling. The surface profile data is used to control the exposure laser intensity to effect surface smoothing via grayscale lithography. In the Figure 7 schematic the exposure wavelength is brought to a focus at a point coinciding with the profilometer's measurement probe point, but it could alternatively be displaced from the measurement point to allow for a data processing delay between the time a surface point is measured and the time it is exposed.

References

[1] Migura, "Optics for EUV lithography," in *2018 EUVL Workshop*, P22, EUV Litho, Inc., https://www.euvlitho.com/2018/P22.pdf

[2] Reichle, R.; Yu, K.; Pruss, C.; Osten, W.: "Spin-coating of photoresist on convex lens substrates," DGAO-Proceedings, ISSN: 1614-8436, 2008. https://www.dgao-proceedings.de/download/109/109_p44.pdf

[3] University of Stuttgart, Institute of Applied Optics. Fabrication of Diffractive Optical Elements using Direct Laser Writing https://www.ito.uni-stuttgart.de/en/research/group-ido/fabrication-of-diffractive-optical-elements/

[4] Smith D, Hausmann DM, inventors; Lam Research Corp, assignee. "EUV photopatterning of vapor-deposited metal oxide-containing hardmasks." United States patent US 9,996,004. 2018 Jun 12. https://patents.google.com/patent/US9996004B2

[5] Voronov DL, Gullikson EM, Padmore HA. "Ultra-low blaze angle gratings for synchrotron and free electron laser applications." *Optics Express.* 2018 Aug 20;26(17):22011-8. https://doi.org/10.1364/OE.26.022011

[6] Siewert F, Löchel B, Buchheim J, Eggenstein F, Firsov A, Gwalt G, Kutz O, Lemke S, Nelles B, Rudolph I, Schäfers F. "Gratings for synchrotron and FEL beamlines: a project for the manufacture of ultra-precise gratings at Helmholtz Zentrum Berlin." *Journal of Synchrotron*

Radiation. 2018 Jan 1;25(1):91-9.
https://doi.org/10.1107/S1600577517015600

[7] "Accurate Tool Servo Control for Precision Diamond Turning using Heterodyne Interferometry." Kenneth C. Johnson, December 2, 2020.
https://vixra.org/abs/2012.0012

[8] Sánchez-López MM, Moreno I, Davis JA, Gutierrez BK, Cottrell DM. "Double-ring interference of binary diffractive axicons." OSA Continuum. 2020 Jun 15;3(6):1679-90.
https://doi.org/10.1364/OSAC.393734

[9] Ksu SK, inventor; Maxoptix Corp, assignee. "Sensor array for focus detection." United States patent US 4,816,665. 1989 Mar 28.
https://patents.google.com/patent/US4816665

[10] Bai Z, Wei J. "Focusing error detection based on astigmatic method with a double cylindrical lens group." Optics & Laser Technology. 2018 Oct 1;106:145-51.
https://doi.org/10.1016/j.optlastec.2018.04.005

August 1, 2021 Addendum

Laser ablation is a material removal process that can be used for surface smoothing of optical glass and mirrors at low to mid-spatial frequencies. (Ref's. 11-14) Also, thermal reflow via laser heating can be used to smooth out high spatial frequencies. (Ref. 15) These processes could be used in conjunction with the above-described interferometric imaging system as an alternative to grayscale lithography. For example, in Figure 7 the exposure laser beam could alternatively be a high-power laser, which smooths the surface via direct laser ablation.

The interferometric system illustrated in Figures 1 and 2 was described above as a heterodyne interferometer, but a more conventional homodyne interferometer could alternatively be used. This might be advantageous for high-speed operation. Also, as noted previously, the surface height measurement at the probe point can be corrected based on the known base surface curvature, but the interferometer can alternatively be designed to provide a measure of the surface curvature over the illumination field. One possible design of this type is illustrated in Figure 8, as described below.

An illumination source such as an optical fiber point source (as illustrated) directs radiation through a collimating lens, through a diffractive surface in the back focal plane of the collimating lens, and then through a focusing lens and onto an inspection surface. The diffracting surface could, for example, be a 2-D Dammann grating. The diffracted light forms an array of focal points on the inspection surface, and light from the focal points is reflected back through the lenses and diffracting surface onto an array of optical detector elements conjugate to the focal points. The detector elements could be optical fiber collectors, which convey radiation to remote sensor elements.

The diffracting surface couples the illumination paths between detector elements, creating optical interference effects that are sensitive to surface height differences between the focal points. For example, Figure 9 illustrates a focused illumination pattern on the inspection surface comprising multiple focused spots such as spot 1 and spot 2. Spot 1 is formed from zero-order (undiffracted) light, and the remaining spots including spot 2 are generated by diffraction at the diffracting surface. Figures 10A and 10B illustrate two optical paths leading from the source to a particular detector element corresponding to spot 2 and giving rise to an interference signal at the detector. In Figure 10A, a portion of the source beam is undiffracted on the first pass through the diffracting surface, is focused to spot 1, and after reflection the beam is diffracted by the diffracting surface and brought to a focus on the detector element. In Figure 10B, the source beam is diffracted on the first pass through the diffracting surface so that it is brought to a focus at spot 2, and the reflected radiation is undiffracted and also brought to a focus on the same detector element. The interference signal at the detector element is sensitive to the height offset between spot 1 and spot 2. As the surface is scanned across the illumination field, the detector signals can be processed to determine the base surface curvature near spot 1 and the surface height of spot 1 relative to the base surface.

Figure 5 illustrates a multilevel confocal focus sensor comprising an illumination fiber and two focus-sensor fibers with different focus offsets. An alternative confocal focus sensor variant, which uses a single fiber for both illumination and collection, is illustrated in Figure 11. The fiber can be a broadband, single-mode fiber, which provides point-source illumination at multiple wavelengths. (For example, Thorlabs Inc. supplies optical fibers of this type, Ref. 16.) The source is focused onto an inspection surface by a chromatically dispersive lens, which could be either a conventional refractive lens, a diffractive (e.g., zone-plate) lens, or a hybrid refractive/diffractive lens (as illustrated). Different wavelengths are brought to a focus at different focal heights proximate the inspection surface (as indicated by the chromatic spread in Figure 11), so the wavelength variation of the return signal collected by the optical fiber provides a sensitive measure of focus height. The lens focal length, and the balance of optical power between the refractive and diffractive surfaces, can be selected to optimize the focus-sensing range and resolution.

The Figure 8 profilometer and the Figure 11 confocal sensor can be combined by using a fiber light source in the Figure 8 configuration for multiwavelength illumination and collection of zero-order, undiffracted light for focus sensing, as in Figure 11. A narrowband optical filter can be located in front of the detector elements to transmit a single wavelength or narrow wavelength band for profilometry.

The above-described surface profiling sensor (Figure 8), focus sensor (Figure 11), and exposure laser beam (for lithographic patterning) can also be combined via beam splitters into a common beam path at the inspection surface, similar to Figure 7. Alternatively, the beam paths can be separated. The “exposure laser beam” can alternatively be replaced by an ablation laser beam for direct surface smoothing and contouring via ablation, or other optical/chemical processes such a laser-induced thermal reflow can be used.

Additional References

[11] PowerPhotonic Ltd. “Laser Ablation Processing (LAP).”
https://www.powerphotonic.com/tools-and-support/technologies/laser-ablation-processing-lap/

[12] Fraunhofer Institute for Laser Technology. “Laser Polishing and Ablation for the Production of Glass Optics.”
https://www.ilt.fraunhofer.de/en/media-center/brochures/brochure-laser-polishing-and-ablation-for-the-production-of-glass-optics-2017.html

[13] Weingarten, Christian, et al. “Laser polishing and laser shape correction of optical glass.” *Journal of laser applications* 29.1 (2017): 011702.
https://doi.org/10.2351/1.4974905

[14] Tamura, Asato, et al. “Picosecond laser ablation on glass using wavelength of 1064, 532, and 355 nm.” *Optical Engineering* 59.7 (2020): 075102.
https://doi.org/10.1117/1.OE.59.7.075102

[15] Wlodarczyk, Krystian L., et al. “Laser smoothing of binary gratings and multilevel etched structures in fused silica.” *Applied optics* 49.11 (2010): 1997-2005.
https://pure.hw.ac.uk/ws/portalfiles/portal/7089713/ao_49_11_1997.pdf

[16] Thorlabs Inc. “Single Mode Optical Fiber.”
https://www.thorlabs.com/navigation.cfm?guide_id=2283

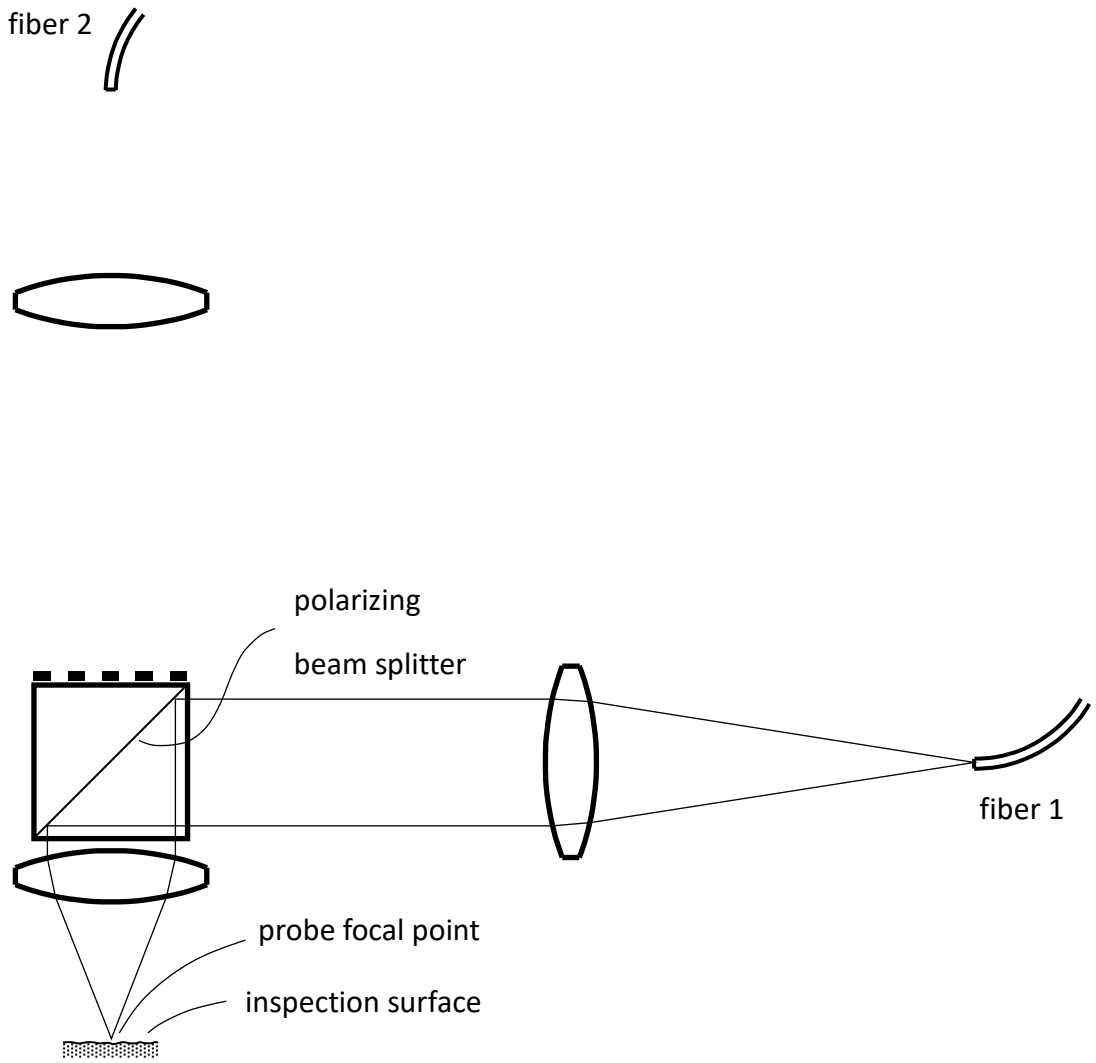
fiber 2
polarizing
beam splitter
fiber 1
probe focal point
inspection surface

Figure 1

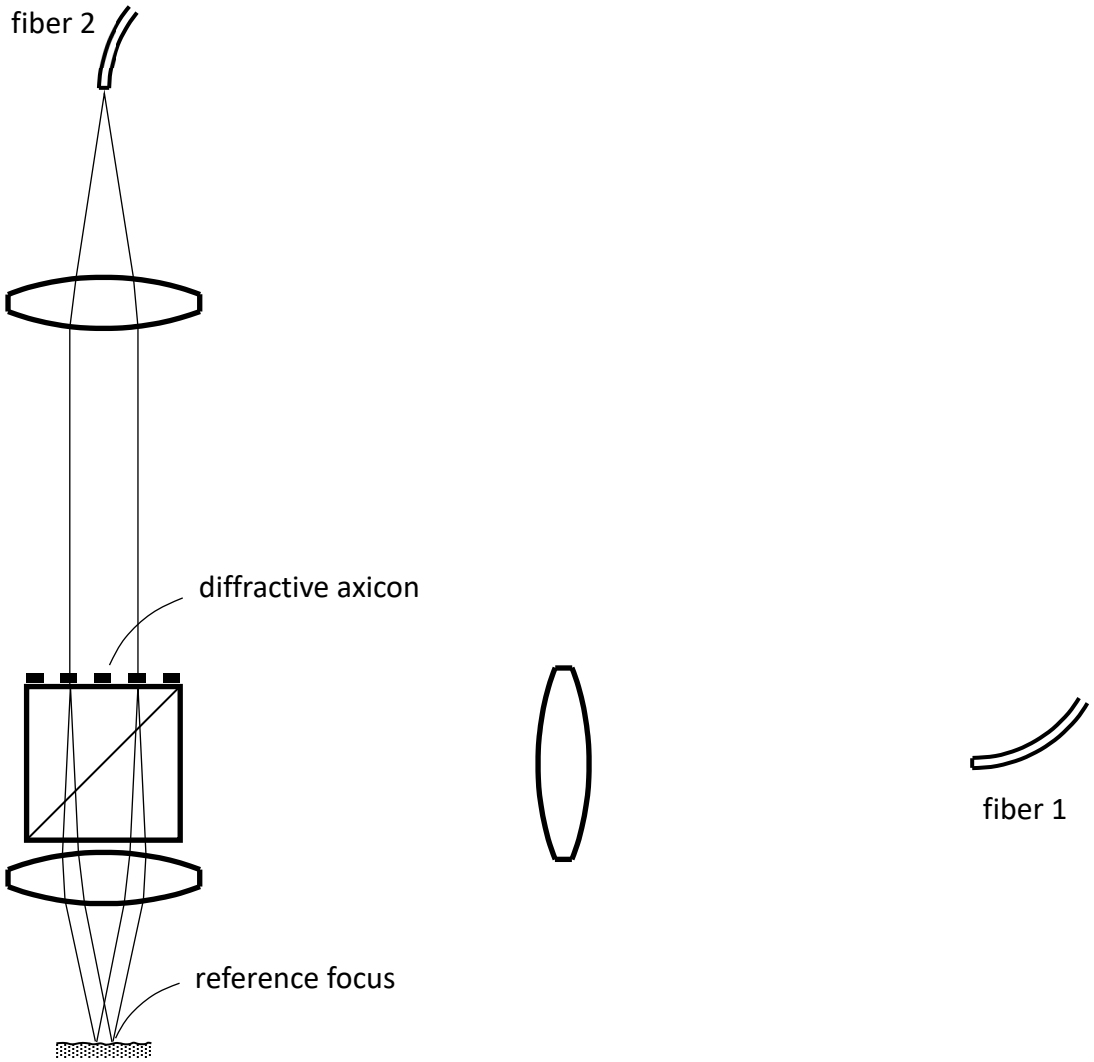

Figure 2

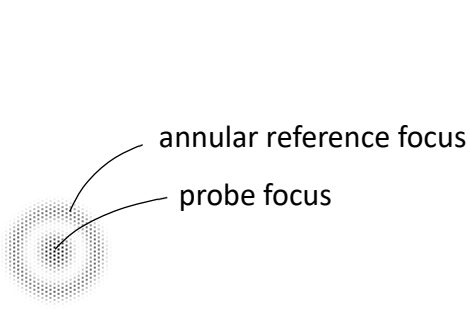

Figure 3

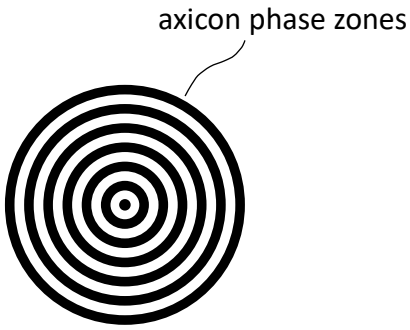

Figure 4

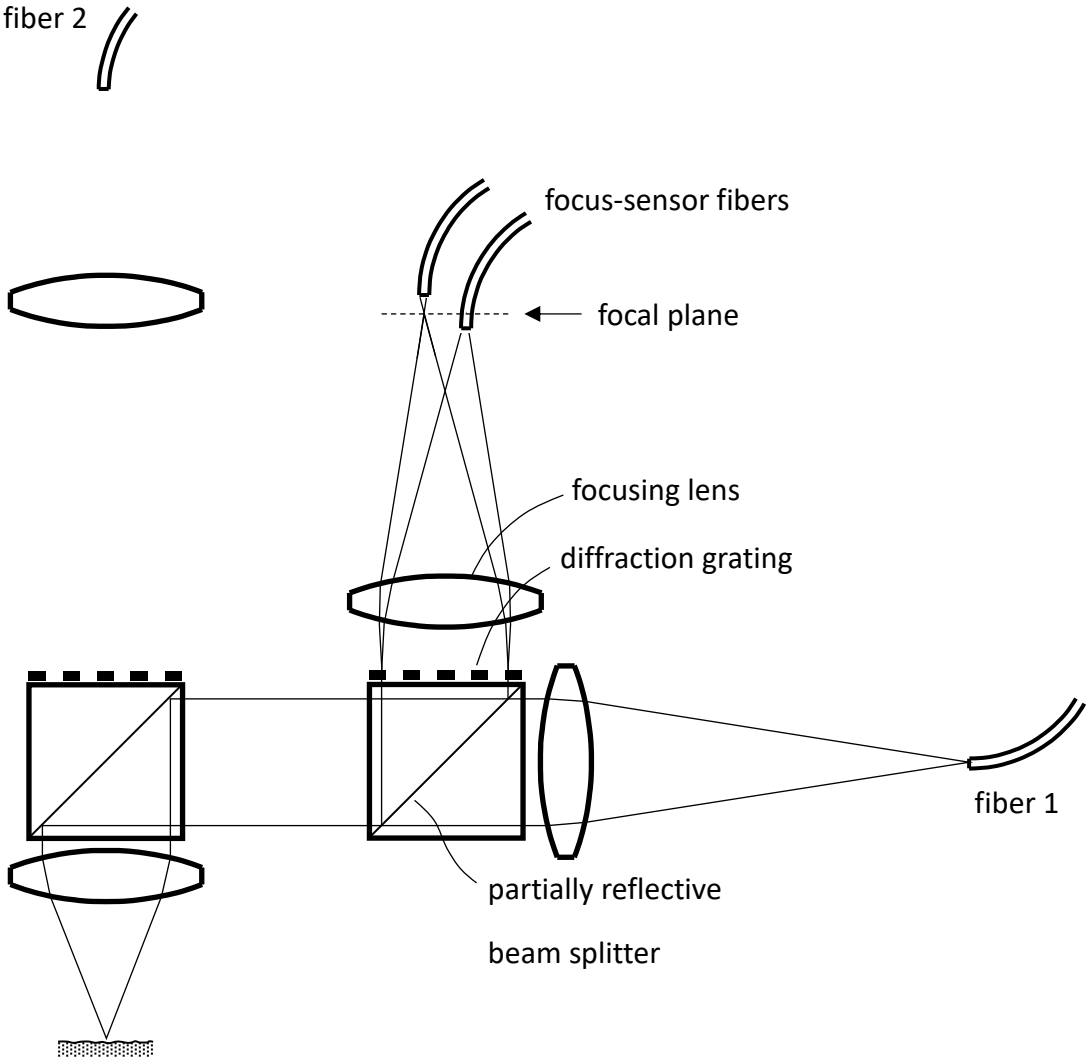

Figure 5

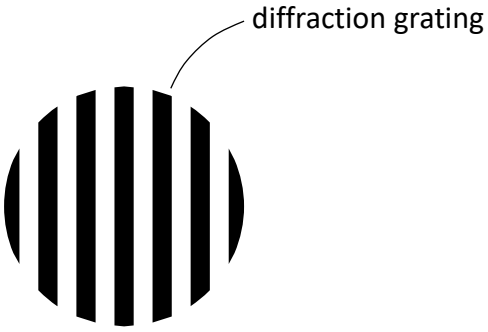

Figure 6

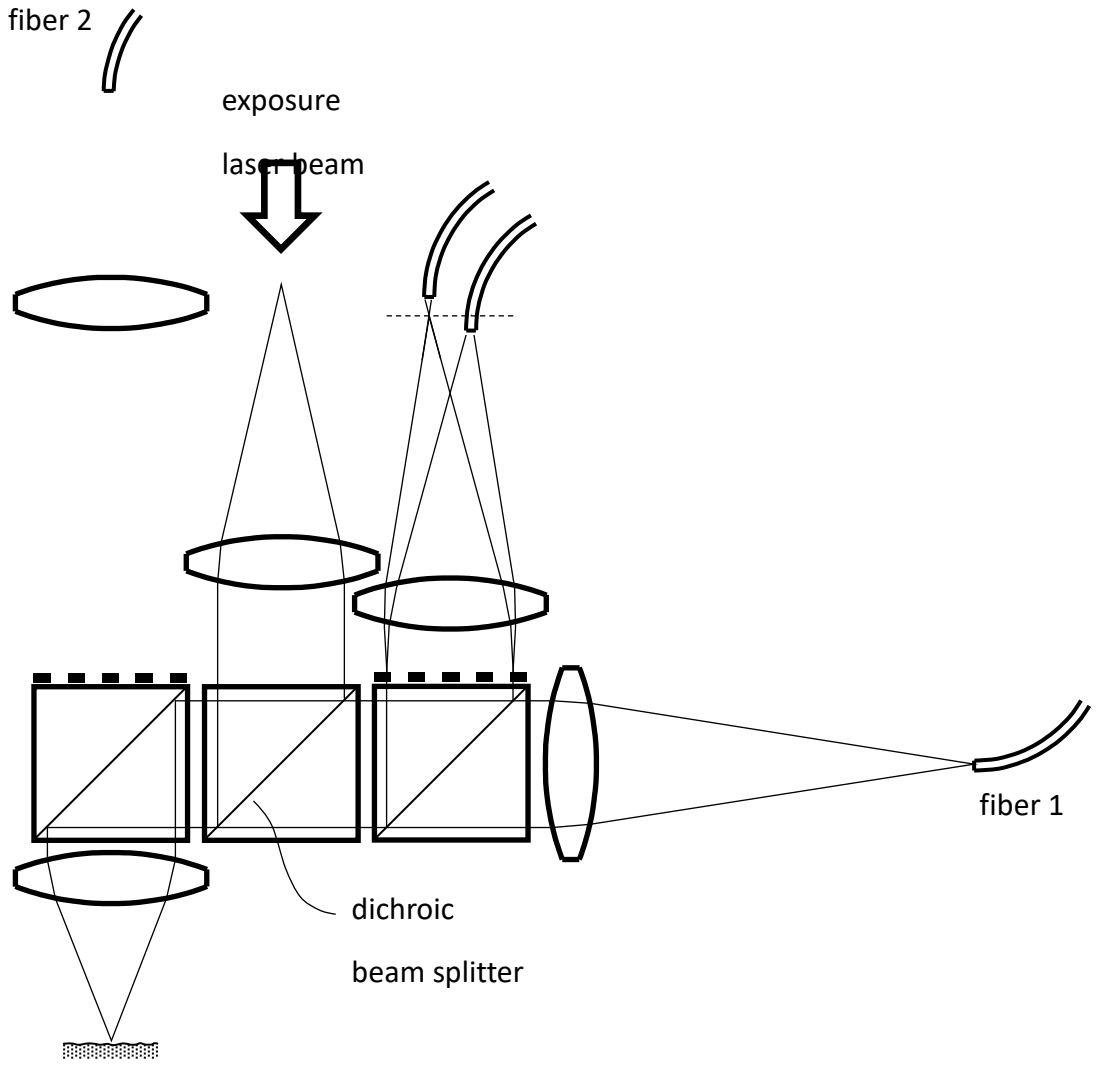

Figure 7

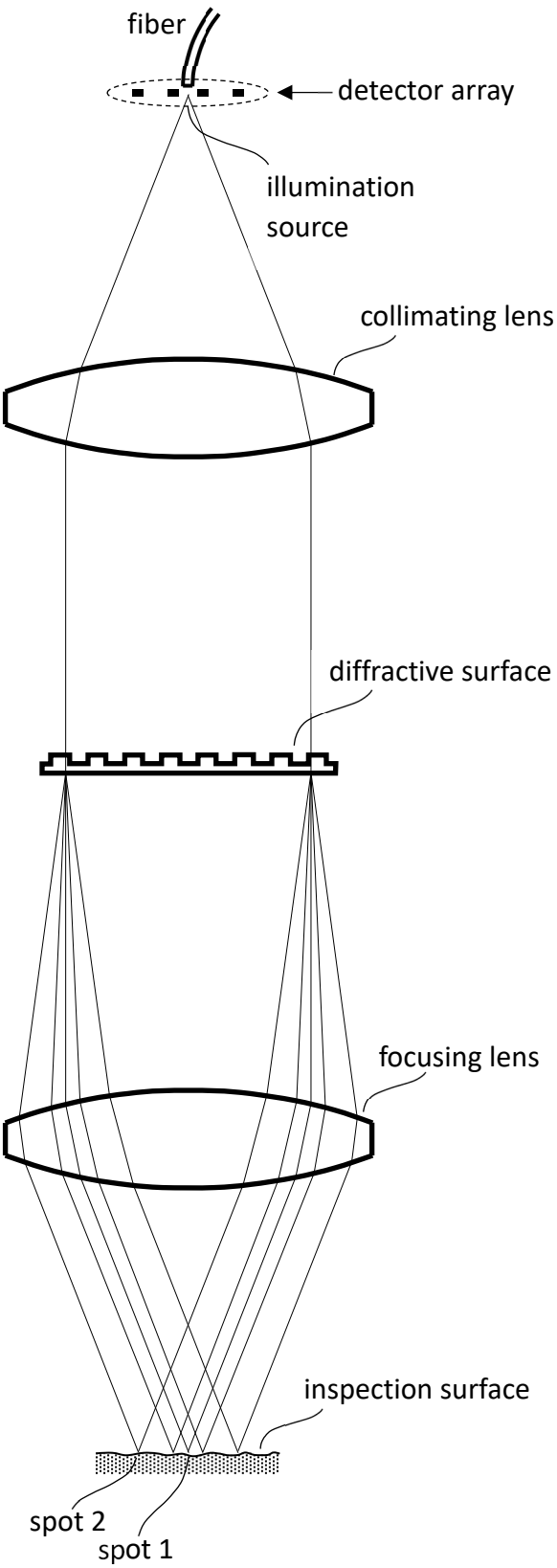

Figure 8

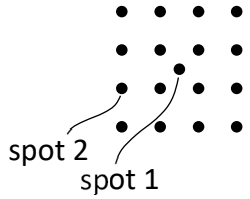

Figure 9

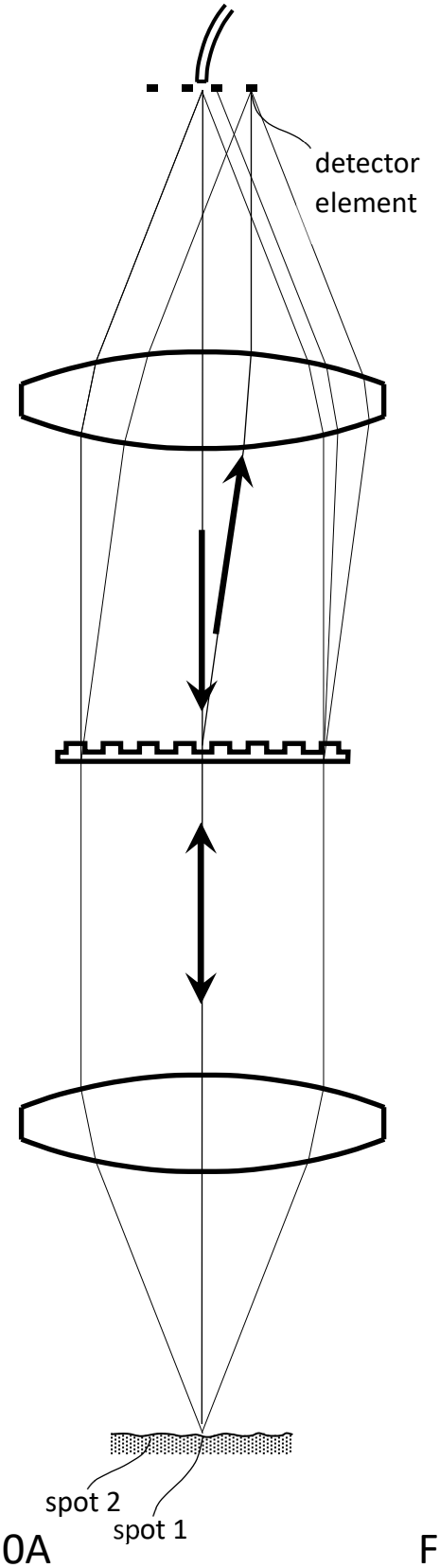

Figure 10A

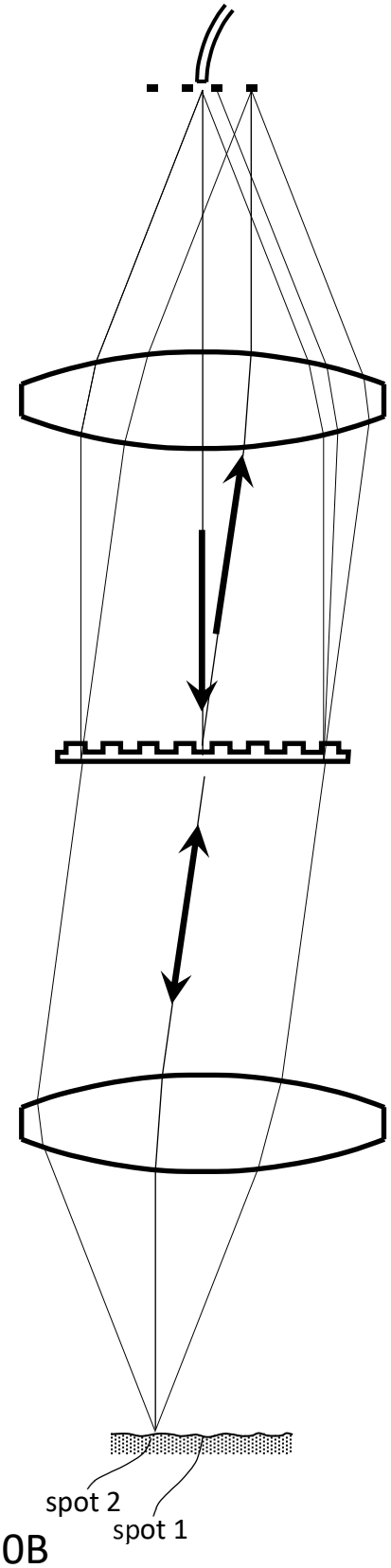

Figure 10B

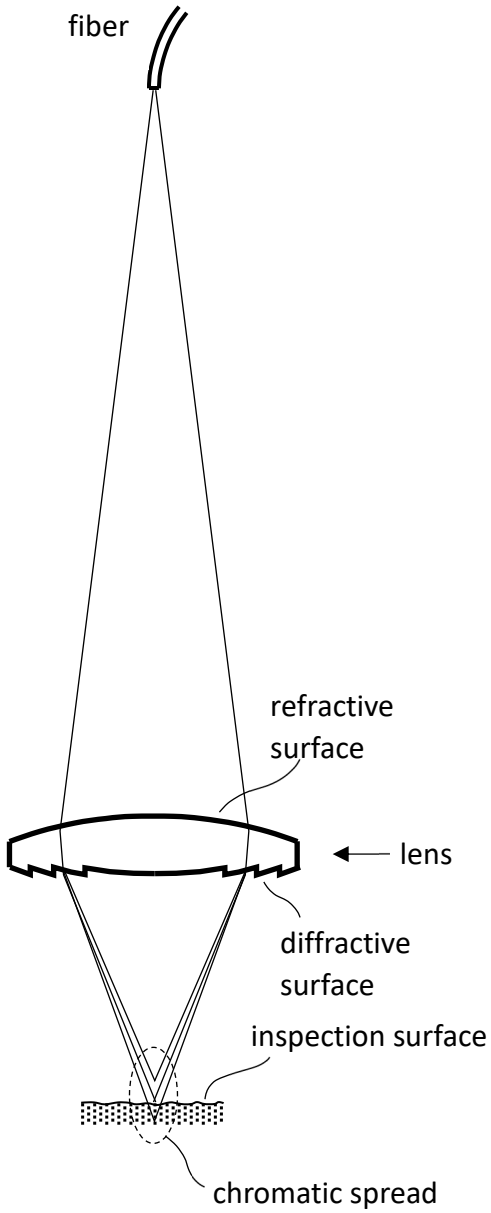
fiber
refractive
surface
lens
diffractive
surface
inspection surface
chromatic spread

Figure 11